

The effect of fast neutron irradiation on the superconducting properties of REBCO coated conductors with and without artificial pinning centers

D X Fischer , R Prokopec, J Emhofer and M Eisterer 

Atominstitut, TU Wien, Stadionallee 2, A-1020 Vienna, Austria

E-mail: david.fischer@tuwien.ac.at

Received 31 October 2017, revised 22 December 2017

Accepted for publication 2 February 2018

Published 7 March 2018



Abstract

Superconductors are essential components of future fusion power plants. The magnet coils responsible for producing the field required for confining the fusion plasma are exposed to considerable neutron radiation. This makes irradiation studies necessary for understanding the radiation response of the superconductor. High temperature superconductors are promising candidates as magnet coil materials. YBCO and GdBCO tapes of several manufacturers were irradiated to fast neutron fluences of up to $3.9 \times 10^{22} \text{ m}^{-2}$ in the research reactor at the Atominstitut. Low energy neutrons contribute to the fission reactor spectrum but not to the expected spectrum at the fusion magnets. Low energy neutrons have to be shielded in irradiation experiments to avoid their substantial effect on the superconducting properties of tapes containing gadolinium. The critical current (I_c) of the tapes in this study was examined at fields of up to 15 T and down to a temperature of 30 K. I_c first increases upon irradiation and reaches a maximum at a certain fluence, which depends highly on temperature, being highest at low temperature. I_c declines at high fluences and eventually degrades with respect to its initial value. Tapes with artificial pinning centers (APCs) degrade at lower fluences than tapes without them. The n -values decrease in all types of tapes after irradiation even when the critical currents are increased. The field dependence of the volume pinning force differs in pristine tapes with and without APCs but shows the same behavior after irradiation.

Keywords: neutron irradiation, coated conductor, pinning force, n -value, transition temperature, disorder effects, critical current

(Some figures may appear in colour only in the online journal)

Introduction

It has been a dream for more than 60 years to use nuclear fusion as a virtually inexhaustible source of energy to produce electricity [1]. Currently, the most promising method is to confine a plasma magnetically in a reactor and heat it up until the fusion process ($D + T \rightarrow \text{He} + n$) takes place at a

satisfactory rate. This requires high magnetic fields (well above 10 T at the magnet position) that can only be provided reasonably by superconducting coils.

The neutrons that result from fusion attain most of the released energy and the majority are absorbed in the blanket and radiation shield. However, a small fraction reach the superconductor where the energy spectrum of the neutrons is broadened by scattering and resembles the high energy part of the neutron spectrum in the TRIGA MARK II research reactor at the Atominstitut.

Hence this facility is suitable for irradiation studies of superconducting magnet components for fusion.



Original content from this work may be used under the terms of the [Creative Commons Attribution 3.0 licence](https://creativecommons.org/licenses/by/3.0/). Any further distribution of this work must maintain attribution to the author(s) and the title of the work, journal citation and DOI.

High temperature superconductors are promising materials for this purpose whereby coated conductors are the most mature technology among them.

Previous studies on neutron irradiated YBCO tapes [2–7] have shown that the anisotropic nature of the superconductor is reduced. Critical currents degrade at lower fluences in the field configuration $H \parallel ab$ than for $H \parallel c$, although the values of I_c remain highest in the direction $H \parallel ab$ [7]. Furthermore, the operating temperature has a significant influence on the radiation robustness—tapes degrade earlier (meaning at lower fluences) if the operation temperature is higher.

Recent efforts of research institutes and manufacturers to improve the performance of coated conductors focus on the inclusion of nanoparticles in the superconducting layer to improve flux pinning [8–14]. These additions have consequences for the radiation resistance of the tapes which is an important factor for fusion magnets. This study addresses this issue by comparing the effects of neutron irradiation on tapes with and without artificial pinning centers.

Samples

We investigated coated conductors from AMSC, SuperPower and SuNAM in this study. All tapes have a width of 4 mm. Pieces of 2.5 cm were cut from the roll and characterized by resistivity measurements.

The AMSC tape 344 C is based on rolling-assisted biaxially textured substrates. The 1.2 μm thick YBCO layer was grown via metal–organic deposition [15]. The tape under study is brass laminated for increased mechanical stability. The SuNAM conductor contains GdBCO deposited using reactive co-evaporation by deposition and reaction as a 1.3 μm superconducting layer with no artificial nanoparticles [16]. Three different types of samples from SuperPower were studied (referred to as SCS4050). All of them have a 1.0 μm thick GdBCO layer which was produced via metal–organic chemical vapor deposition on an ion beam assisted deposition MgO layer [17]. Two different generations (the more recent one from 2013) contain artificial pinning centers for improved flux pinning. They are denoted by SCS4050-AP.

Methods

All results were obtained from transport current measurements in a 17 T helium flow cryostat with the field applied perpendicular to the tape surface using a four-terminal technique. The current leads were connected to the sample via indium press contacts. Two pogo pins were dipped into conductive silver and pressed onto the tape for sensing the voltage drop along a distance of 2.5 mm. The current was ramped up during the measurement until an abort criterion of around 6 μV was reached. The resulting IV -curves were evaluated by a linear fit in the double logarithmic plot and using an electric field criterion of 1 $\mu\text{V cm}^{-1}$. The slope of these curves defines the n -value.

The data for the irreversibility lines (IL) were obtained by ramping the temperature down at a constant rate of 13 K h^{−1}

while measuring the voltage at the superconductor resulting from a current of 10 mA in variable background fields of up to 15 T. The extrapolation of the tangent at the middle of the transition to zero defines the temperature at which the applied field becomes the irreversibility field B_{irr} .

To obtain the transition temperature, T_c , the transition tangent was intersected with the linear extrapolation of the normal state behavior in zero field.

After an initial characterization, the samples were irradiated in the TRIGA MARK II research reactor at the Atominsitut. The neutron spectrum in the center of the core where the irradiation took place has two peaks in the lethargy representation (lethargy $u = \ln(E_0/E)$, $E_0 = 10$ MeV)—one below 0.1 eV and the other at around 1 MeV [18]. The neutron flux density of low energy neutrons ($E_{\text{kin}} < 0.55$ eV) accounts for 29% of the total flux density while fast neutrons ($E_{\text{kin}} > 0.1$ MeV) contribute 36%. All fluences given in this work refer to fast neutrons.

The neutron energy distribution in our irradiation facility differs from the spectrum expected at fusion magnets mainly due to the negligible contribution of thermal neutrons in the latter [19]. While these low energy neutrons had hardly any effect on the superconducting properties of YBCO tapes [4], they had a severe impact in the case of GdBCO [5] as will be shown in the following section. This is attributable to the large cross section of two gadolinium isotopes (Gd-155 and Gd-157, $\sim 15\%$ natural abundance each) for capturing thermal neutrons [20]. To avoid the significant and unwanted influence of low energy neutrons, the GdBCO tapes were, unless otherwise stated, wrapped in cadmium foil to shield these thermal neutrons.

The tapes were sealed in quartz glass tubes before the irradiation together with a thin nickel foil that was used to monitor the fast neutron fluence. After the irradiation process and months of decay time, the samples were ready to be handled for experimental investigation. Several of these ‘irradiation—cool down—measuring’ steps have been performed on the tapes.

The samples were irradiated to a cumulative neutron fluence of up to $3.9 \times 10^{22} \text{ m}^{-2}$. For comparison, the design fluence of ITER is 10^{22} m^{-2} . The mechanical strength of a suitable electrical insulation material (pure cyanate ester and mixtures with epoxies) has been studied up to a fluence of $5 \times 10^{22} \text{ m}^{-2}$ [21]. The radiation robustness of the insulation material sets another limit for the fluence the magnet coils can withstand.

The physical properties of superconductors are altered by neutron irradiation because of the defects that are introduced in the microstructure of the material. These defects vary in type and size. Point defects are, due to their small size, difficult to detect. They have been studied using positron annihilation lifetime spectroscopy [22]. Point defects can move relatively easily (e.g. thermally activated) and may form clusters. Another important process is the formation of collision cascades, caused by high energy primary knockout atoms. These defects are comparable in size with the coherence length of YBCO and, therefore, act as strong pinning centers. Collision cascades were examined using transmission electron microscopy [23].

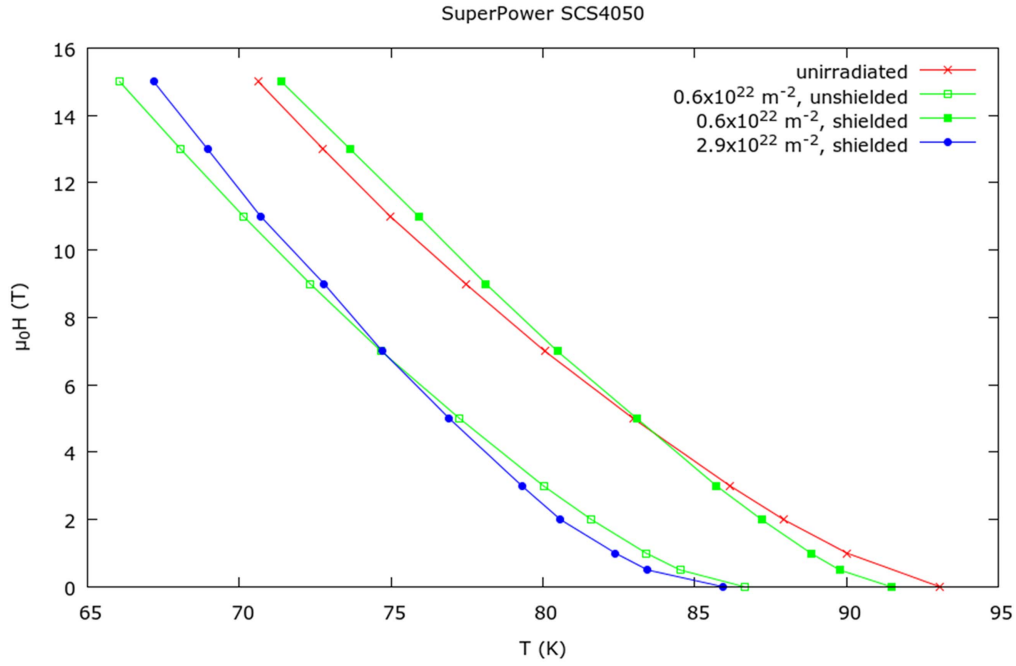


Figure 1. Effect of low energy neutrons on the irreversibility line of a GdBCO tape.

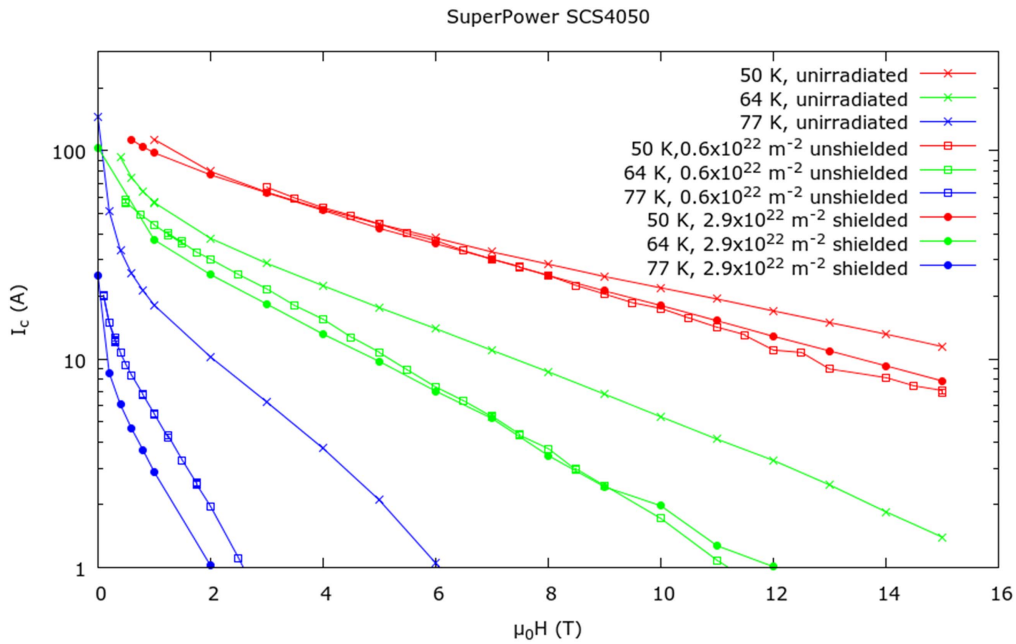


Figure 2. Critical currents in an irradiated GdBCO tape—unshielded: $0.6 \times 10^{22} \text{ m}^{-2}$, shielded: $2.9 \times 10^{22} \text{ m}^{-2}$.

Results

Low energy neutrons

Figure 1 demonstrates the effect of low energy neutrons on the IL of a GdBCO tape (SCS4050 from SuperPower) by comparing data after irradiation with and without a cadmium shield.

The crosses refer to the pristine tape, the open squares result after exposure to the full reactor spectrum, the solid squares and circles represent the data after irradiation to the same fast neutron fluence, but without the low energy part of

the neutron spectrum which was absorbed in a cadmium foil that surrounded the sample. After irradiation to the same fluence ($0.6 \times 10^{22} \text{ m}^{-2}$), the transition temperature drops by 1.6 K in the shielded tape (solid squares) and by considerable 6.3 K in the unshielded sample (open squares). A similar T_c reduction (7.0 K) results in the shielded case at a much higher fluence of $2.9 \times 10^{22} \text{ m}^{-2}$ (solid circles).

Since the T_c degradation is very similar in the latter two cases (unshielded irradiation at $0.6 \times 10^{22} \text{ m}^{-2}$ and shielded irradiated at $2.9 \times 10^{22} \text{ m}^{-2}$), it is interesting to compare the corresponding critical currents. While they are higher by a

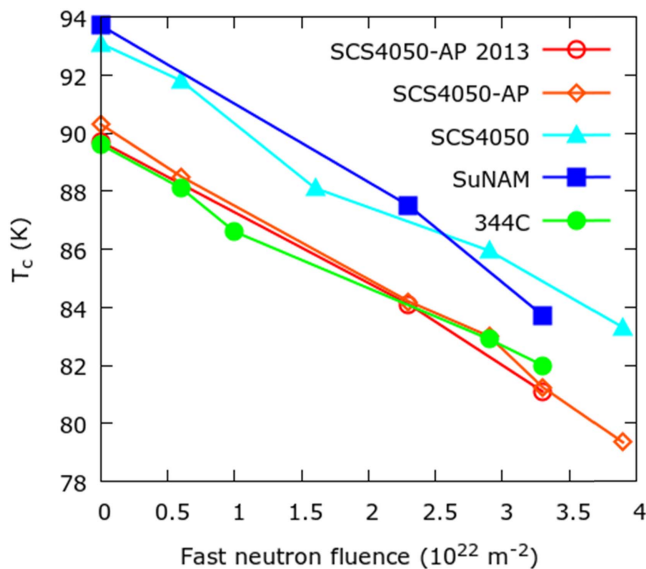


Figure 3. Fluence dependence of the critical temperature in various coated conductor tapes.

factor of 1.8 in the unshielded tape at 77 K (blue curves in figure 2), the differences in I_c of these two cases are very small at lower temperatures (64 and 50 K, green and red data points).

At all temperatures, the critical currents dropped below their initial values, so the irradiation exceeded the fluence where I_c has the maximum value (more on the fluence dependent I_c behavior in the next section).

The two samples from the same tape have very similar critical currents, although the radiation induced defect structure is completely different. The shielded sample was exposed to a five times higher fast neutron fluence so it has a five times higher density of collision cascades. The predominant defects in the unshielded sample are point defects of displaced gadolinium atoms [5]. After the capture of a thermal neutron, the relaxation from the excited state of the gadolinium nucleus produces gamma radiation having a recoil energy of around 30 eV [24], just enough to displace this gadolinium atom.

It is not unexpected that a high density of point-like disorder significantly affects T_c . It is surprising on the other hand, that the large difference in the number of defect cascades, which are believed to be the most efficient pinning centers after irradiation, does not influence I_c . It has to be noted that the critical currents dropped below their initial values, so the irradiation exceeded the fluence where I_c has its maximum (more on the fluence dependent I_c behavior in the next section), hence the density of defects is too high for optimized pinning in either case. Further studies are necessary to clarify the reasons for the observed similar changes in T_c and I_c despite the differences in the underlying defect structure, in particular, if this behavior also prevails at low neutron fluences, where I_c is increased with respect to the pristine tape.

High energy neutrons

The transition temperatures of the coated conductors decrease in all tapes after neutron irradiation, as shown in figure 3. The

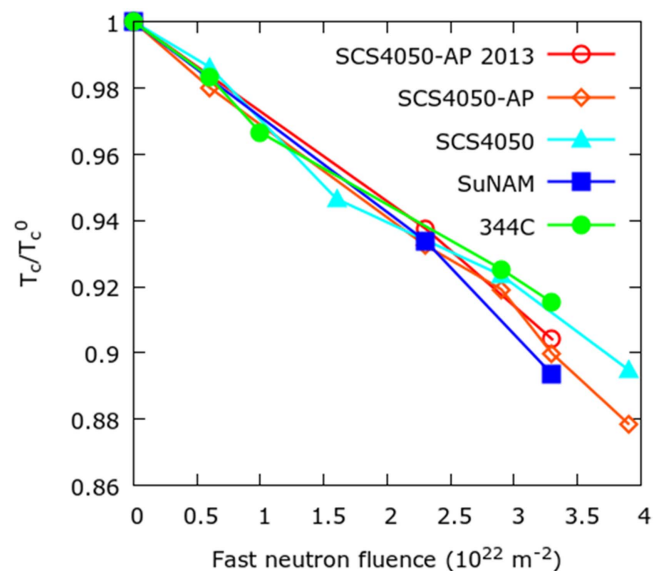


Figure 4. Data from figure 3 as a function of the normalized critical temperature.

fluence dependence of the reduced temperature shows almost a universal behavior (decline of $\sim 3\%$ per 10^{22} m^{-2}) as can be seen in figure 4.

In contrast to the transition temperature, the fluence dependence of the critical current is non-monotonic. At low neutron fluences, the introduced defects improve flux pinning and the critical currents increase. However, at a certain defect density the critical current reaches its maximum and I_c declines upon further irradiation. This defect density dependent behavior is also seen in computer simulations using a time dependent Ginzburg–Landau model [25]. The exact physical mechanism behind this phenomenon will be the subject of further research.

The dependence of the critical currents on the neutron fluence in a YBCO tape is shown in figure 5. The data were obtained in a background field of 15 T oriented perpendicular to the tape surface. The point of degradation, defined as the fluence at which the critical current drops below its initial value, is highly temperature dependent. This behavior is found to be universal and not specific to a certain tape—all studied tapes degrade earlier (i.e. at a lower neutron fluence) at higher temperatures.

It is interesting to compare the radiation robustness of tapes with and without artificial pinning centers. Figure 6 shows the enhancement factor (critical currents normalized by its pre-irradiation values) of the tapes at 30 K and a field of 15 T ($H \parallel c$).

It is striking that the critical currents in tapes with artificial pinning centers (SCS4050-AP, open circles and diamonds in figure 6) drop below their initial values at lower neutron fluences than in tapes without APCs.

It can be assumed that the critical currents degrade at a certain defect density (for a given temperature). It is thus understandable that tapes with APCs having a higher initial defect density can only withstand less radiation damage, as illustrated in figure 7.

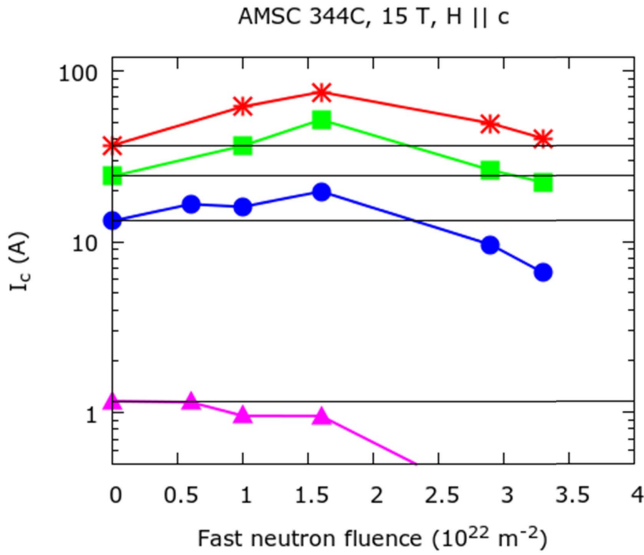


Figure 5. Fluence dependence of the critical current in a YBCO tape for several temperatures. Most data were previously published in [6].

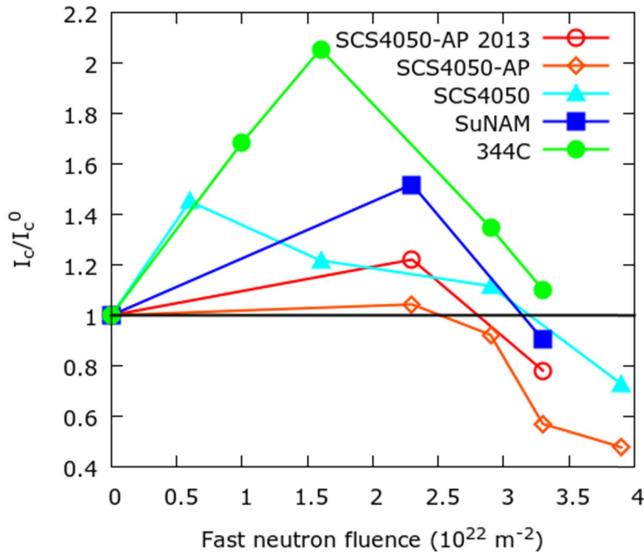


Figure 6. Fluence dependent I_c -enhancement factor of several coated conductors at 30 K, 15 T ($H \parallel c$).

The absolute values of the critical currents are shown in figure 8, since they are practically more important than the relative changes. The uppermost (green) curve represents the results of the more recent GdBCO tape with artificial pinning centers. Although the critical currents decline at lower neutron fluence than in ‘clean’ tapes, I_c of this tape is still highest in the entire investigated fluence range.

Changing in pinning are also reflected by the n -value, which is associated with the activation energy needed to remove the vortex from the pin. A higher value corresponds to stronger individual pinning centers. The n -values and critical currents are shown before and after irradiation in figure 9. After irradiating the tapes to $2.3 \times 10^{22} \text{ m}^{-2}$, the critical currents at 40 K are higher than initially in both tapes,

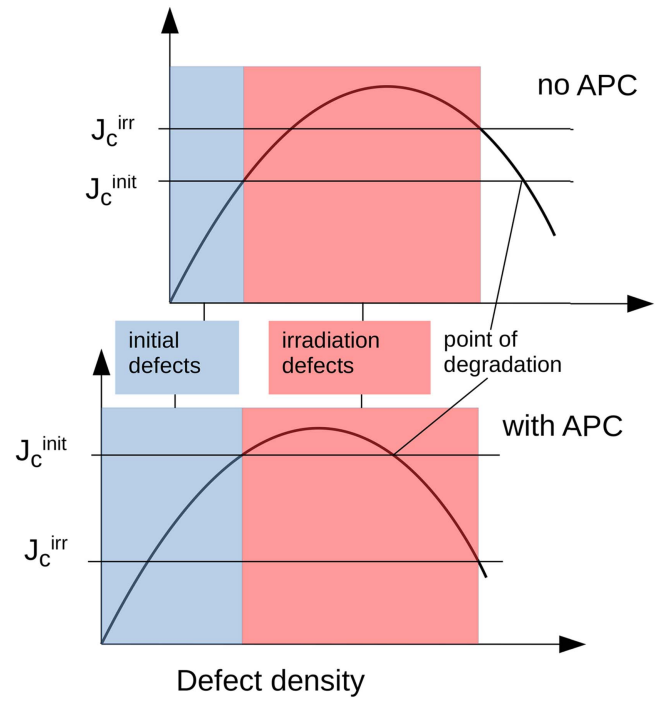


Figure 7. Sketch of the critical current densities in tapes without and with artificial pinning centers. The latter have a higher critical current density J_c^{init} in the beginning caused by a larger initial defect density. After irradiation, the critical current density J_c^{irr} degrades in this example ($J_c^{\text{init}} > J_c^{\text{irr}}$) while for a tape without APCs the critical current density is enhanced after irradiation to the same fluence.

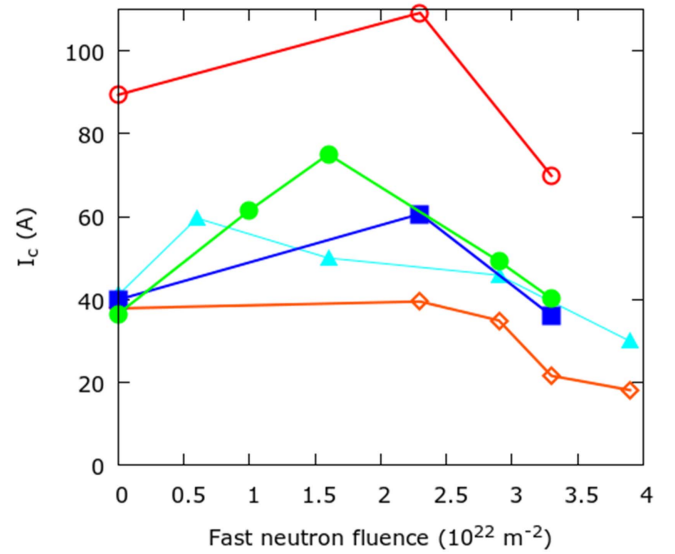


Figure 8. Fluence dependence of critical currents in various tapes at 30 K, 15 T ($H \parallel c$). Same symbols as in figure 6 are used.

although the increase is larger in the tape without artificial pinning centers. Despite the enhancement in I_c , the n -values are lower than before irradiation in both tapes. At 50 K, the critical currents are increased after irradiation in the tape without APC, while I_c degrades in the tape with APC. Nevertheless, the n -value is reduced in either case. Further

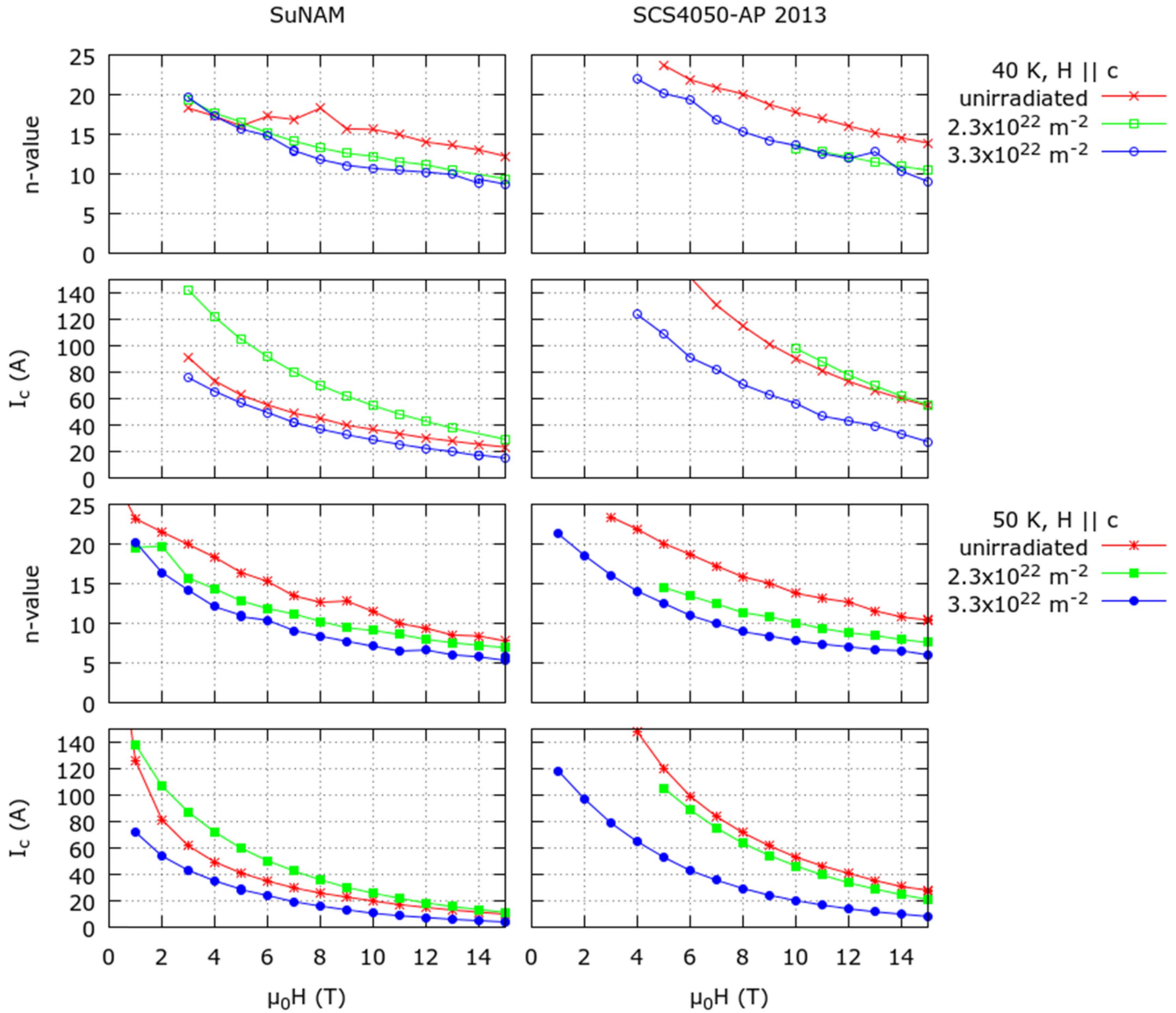


Figure 9. n -values and critical currents in tapes without APCs (left, SuNAM) and with APCs (right SCS4050-AP 2013 from SuperPower).

irradiation of the tapes to $3.3 \times 10^{22} \text{ m}^{-2}$ leads to I_c degradation of both tapes at 40 and 50 K. The n -value is hardly changed compared to the previous irradiation step at 40 K, but the decline is considerable at 50 K.

The field dependent volume pinning force $F_p(B) = J_c(B) \cdot B$ holds information about the type of pinning that is dominant. The magnetic field is commonly normalized by a scaling field, for example the upper critical field B_{c2} . Theoretical considerations predict different positions of the maximum of the pinning force curve in this representation depending on the pinning mechanism [26]. Irradiation to neutron fluences occurring in our studies induce dilute defects in the superconductor. Campbell and Evetts predict in this case of dilute pinning centers the position of the pinning force maximum at a reduced field of 0.2, using B_{c2} as scaling field [27].

In high temperature superconductors B_{c2} is not the appropriate scaling field, instead the irreversibility field B_{irr} is often used. To study the normalized volume pinning force, $B_{irr}(T)$ was obtained by fitting the function $B_{irr}(T) = B_{irr}(0) \cdot (1 - T/T_c)^n$ to

the ILs. Figures 10 and 11 show the experimental data and the corresponding fit functions.

Since the IL could be measured only up to 15 T, the function $B_{irr}(T)$ has to be extrapolated to low temperatures. It will be used down to temperatures of 50 K where it is considered as a reasonable approximation, resulting in scaling fields of up to about 40 T.

Figures 12 and 13 show the normalized volume pinning force as a function of the normalized magnetic field.

The shape of the pinning curves become extremely similar after irradiation for both kind of tapes (with and without APCs) and for both fluences (green triangles and blue squares). At 50 K, the two unirradiated tapes (red circles) have clearly different pinning properties. Their difference vanishes after irradiation, which is a hint that pinning is dominated by the induced defects after irradiation and the initial pinning structure only plays a minor role. The position of the pinning force maximum is close to the predicted value for dilute pins [27].

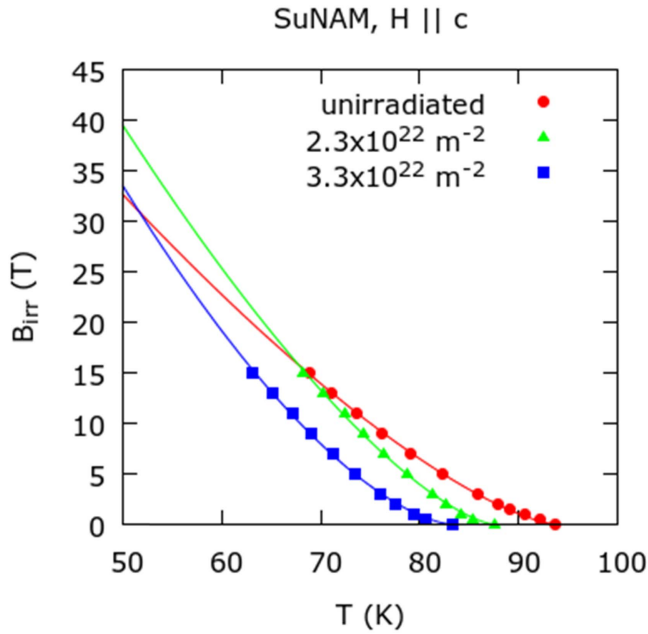


Figure 10. Irreversibility line of a tape without APCs. The line graphs represent fit functions defined in the text.

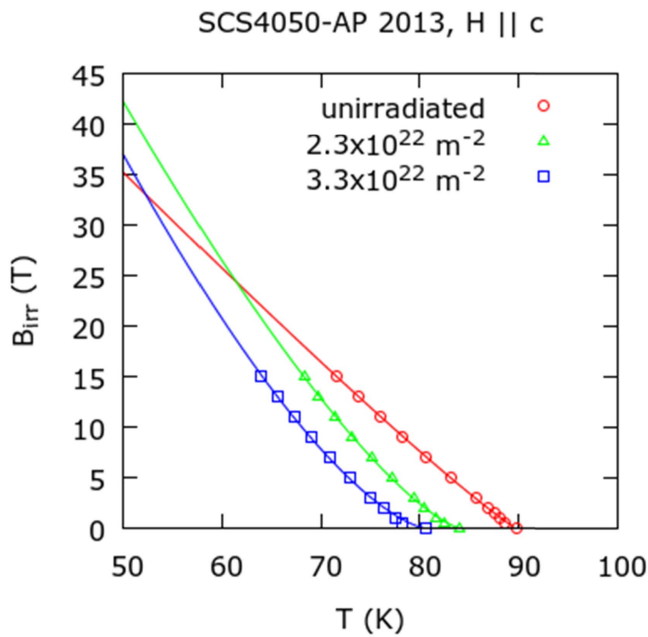


Figure 11. Same as in figure 10 but for a tape with APCs.

Conclusions

Irradiation of GdBCO tapes with low energy neutrons has a severe impact on the superconductor. These neutrons can effectively be shielded if the tapes are wrapped into a cadmium foil during the irradiation process. Without this measure, the T_c degradation is around five times higher and not representative for the situation in a fusion reactor.

The effect of artificial pinning centers on the radiation robustness of coated conductors is different for the different superconducting properties. While the critical temperature

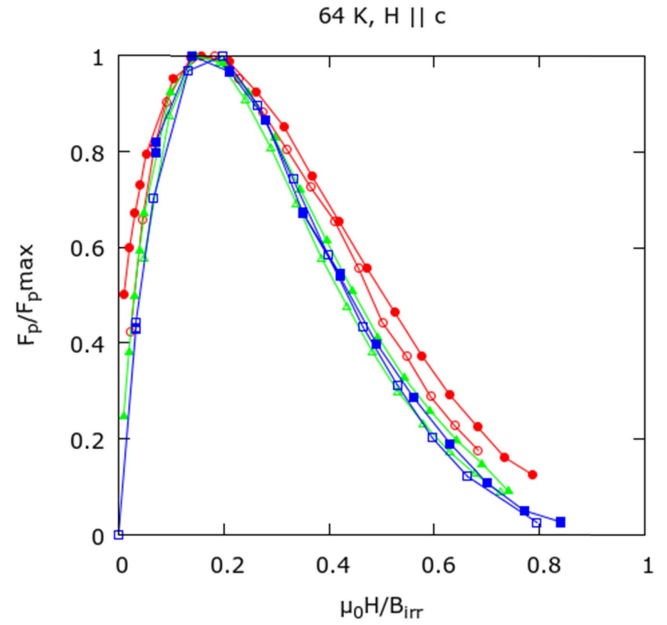


Figure 12. Normalized volume pinning force at 64 K. Same symbols as in figure 13 are used.

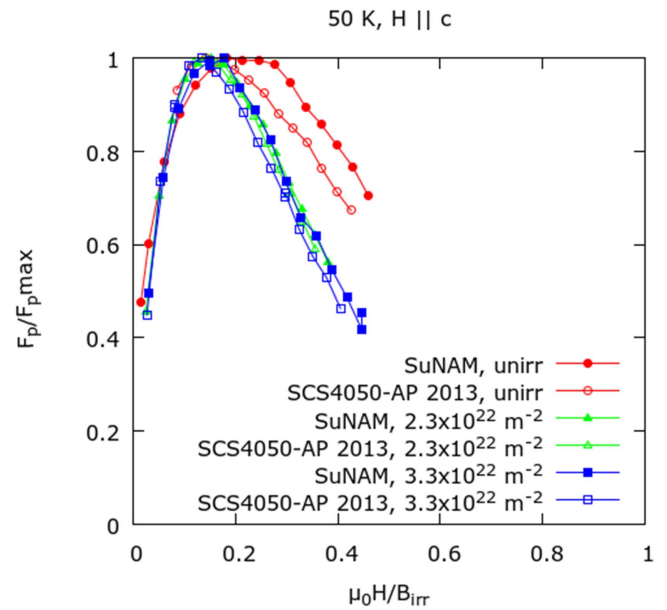


Figure 13. Normalized volume pinning force at 50 K.

declines with increasing neutron fluence for all kinds of tapes at the same rate ($\sim 3\%$ per 10^{22} m^{-2}), the behavior of the critical currents depends on the presence of APCs. Tapes with artificial pinning centers degrade at a lower fluence than tapes without APCs.

The volume pinning force, holding information about the pinning mechanism in superconductors, has a different field dependence in tapes with and without APCs prior to irradiation. These differences vanish at a fluence of $2.3 \times 10^{22} \text{ m}^{-2}$ and further irradiation does not change the shape of the volume pinning force anymore. It can be concluded that the pinning mechanism is dominated by

the induced defects after irradiation, regardless if the tape originally contained APCs.

Acknowledgments

This work has been carried out within the framework of the EUROfusion Consortium and has received funding from the Euratom research and training programme 2014–2018 under grant agreement No. 633053. The views and opinions expressed herein do not necessarily reflect those of the European Commission.

The authors acknowledge the TU Wien University Library for financial support through its Open Access Funding Programme.

We want to thank the manufacturers AMSC, SuNAM and SuperPower for providing us with samples of their coated conductor tapes. Furthermore we want thank David Keays for proof-reading this paper.

ORCID iDs

D X Fischer  <https://orcid.org/0000-0003-2916-8555>

M Eisterer  <https://orcid.org/0000-0002-7160-7331>

References

- [1] Braams C M and Stott P E 2002 *Nuclear Fusion: Half a Century of Magnetic Confinement Fusion Research* (Bristol: Institute of Physics Publishing)
- [2] Fuger R, Eisterer M and Weber H W 2009 YBCO coated conductors for fusion magnets *IEEE Trans. Appl. Supercond.* **19** 1532
- [3] Eisterer M, Fuger R, Chudy M, Hengstberger F and Weber H W 2010 Neutron irradiation of coated conductors *Supercond. Sci. Technol.* **23** 014009
- [4] Chudy M, Fuger R, Eisterer M and Weber H W 2011 Characterization of commercial YBCO coated conductors after neutron irradiation *IEEE Trans. Appl. Supercond.* **21** 3162
- [5] Emhofer J, Eisterer M and Weber H W 2013 Stress dependence of the critical currents in neutron irradiated (RE) BCO coated conductors *Supercond. Sci. Technol.* **26** 035009
- [6] Prokopec R, Fischer D X, Weber H W and Eisterer M 2015 Suitability of coated conductors for fusion magnets in view of their radiation response *Supercond. Sci. Technol.* **28** 014005
- [7] Jirsa M, Rameš M, Ďuran I, Melišek T, Kováč P and Viererbl L 2017 Electric currents in REBaCuO superconducting tapes *Supercond. Sci. Technol.* **30** 045010
- [8] Foltyn S R, Civalé L, MacManus-Driscoll J L, Jia Q X, Maiorov B, Wang H and Maley M 2007 Materials science challenges for high-temperature superconducting wire *Nat. Mater.* **6** 631
- [9] Maiorov B, Baily S A, Zhou H, Ugurlu O, Kennison J A, Dowden P C, Holesinger T G, Foltyn S R and Civalé L 2009 Synergetic combination of different types of defect to optimize pinning landscape using BaZrO₃-doped YBa₂Cu₃O₇ *Nat. Mater.* **8** 398
- [10] Matsumoto K and Mele P 2009 Artificial pinning center technology to enhance vortex pinning in YBCO coated conductors *Supercond. Sci. Technol.* **23** 014001
- [11] Erbe M *et al* 2015 BaHfO₃ artificial pinning centres in TFA-MOD-derived YBCO and GdBCO thin films *Supercond. Sci. Technol.* **28** 114002
- [12] Selvamanickam V, Heydari Gharahcheshmeh M, Xu A, Galstyan E, Delgado L and Cantoni C 2015 High critical currents in heavily doped (Gd,Y)Ba₂Cu₃O_x superconductor tapes *Appl. Phys. Lett.* **106** 032601
- [13] Sueyoshi T, Sogo T, Nishimura T, Fujiyoshi T, Mitsugi F, Ikegami T, Awaji S, Watanabe K, Ichinose A and Ishikawa N 2016 Angular behaviour of critical current density in YBa₂Cu₃O_y thin films with crossed columnar defects *Supercond. Sci. Technol.* **29** 065023
- [14] Wu J and Shi J 2017 Interactive modeling-synthesis-characterization approach towards controllable *in situ* self-assembly of artificial pinning centers in RE-123 films *Supercond. Sci. Technol.* **30** 103002
- [15] Rupich M W, Li X, Sathyamurthy S, Thieme C L H, DeMoranville K, Gannon J and Fleshler S 2013 Second generation wire development at AMSC *IEEE Trans. Appl. Supercond.* **23** 6601205
- [16] Lee J-H, Lee H, Lee J-W, Choi S-M and Moon S-H 2014 RCE-DR, a novel process for coated conductor fabrication with high performance *Supercond. Sci. Technol.* **27** 044018
- [17] Xiong X, Kim S, Zdun K, Sambandam S, Rar A, Lenseth K P and Selvamanickam V 2009 Progress in high throughput processing of long-length, high quality, and low cost IBAD MgO buffer tapes at superpower *IEEE Trans. Appl. Supercond.* **19** 3319
- [18] Weber H W, Böck H, Unfried E and Greenwood L R 1986 Neutron dosimetry and damage calculations for the TRIGA MARK-II reactor in Vienna *J. Nucl. Mater.* **137** 236
- [19] Weber H W 2011 Radiation effects on superconducting fusion magnet components *Int. J. Mod. Phys. E* **20** 1325
- [20] Kopecky J, Sublet J-C, Simpson J A, Forrest R A and Nierop D 1997 Atlas of Neutron Capture Cross Sections (IAEA) www-nds.iaea.org/ngatlas2
- [21] Prokopec R, Humer K, Maix R K, Fillunger H and Weber H W 2010 Characterization of advanced cyanate ester/epoxy insulation systems before and after reactor irradiation *Fusion Eng. Des.* **85** 227
- [22] Chudy M, Eisterer M, Weber H W, Veterníková J, Sojak S and Slugeň V 2012 Point defects in YBa₂Cu₃O_{7-x} studied using positron annihilation *Supercond. Sci. Technol.* **25** 075017
- [23] Frischherz M C, Kirk M A, Farmer J, Greenwood L R and Weber H W 1994 Defect cascades produced by neutron irradiation in YBa₂Cu₃O_{7-δ} *Physica C* **232** 309
- [24] Sickafus K E, Willis J O, Kung P J, Wilson W B, Parkin D M, Maley M P, Clinard F W Jr, Salgado C J, Dye R P and Hubbard K M 1992 Neutron-radiation-induced flux pinning in Gd-doped YBa₂Cu₃O_{7-x} and GdBa₂Cu₃O_{7-x} *Phys. Rev. B* **46** 11862
- [25] Koshelev A E, Sadovskyy I A, Phillips C L and Glatz A 2016 Optimization of vortex pinning by nanoparticles using simulations of the time-dependent Ginzburg–Landau model *Phys. Rev. B* **93** 060508
- [26] Dew-Hughes D 1974 Flux pinning mechanisms in type II superconductors *Phil. Mag.* **30** 293
- [27] Campbell A M and Evetts J E 1972 Critical currents in superconductors *Adv. Phys.* **21** 199